WP1.1 Structure of representative samples: Zuidwending cavern field

by MaP and Geostructures

Version 221027

Contractor: Nobian Industrial Chemicals B.V.

27 October 2022

Contributors:

[redacted] 5.1.2.e [redacted]

[1]MaP Microstructures and Pores GmbH

[2]**Geo**Structures Consultancy for Structural geology and Geomechanics, Maastricht

Reviewed by:

5.1.2.e [redacted]

[3]Brouard Consulting

[4]smartTectonics

Contents

Summary

This report describes the sampling procedure of 27 core pieces for analyses, experiments, and numerical models in the subsequent work packages.

The introduction summarizes the aim of the selection and sampling procedure along with a brief overview of the core material available and the field area. Chapter two describes the methodology in further detail. A qualitative description and quantitative analysis of core slab composition and lithotypes is summarized in the next chapter. The last chapter describes the selection criteria and outcome of the core piece selection for the microstructural analyses, deformation and permeation experiments.

A complete overview of all selected cores, slabs, slab segmentations and selection of sub-samples for microscale analyses deformation and permeation experiments is presented in Appendix A. The initial core selection was based on the core photographs in reflected and transmitted light available on the *Nederlands Olie- en Gasportaal* website[1]. The collection of these photographs is listed in Appendix B.

We started by reviewing the end of well report, the core photos and the core description and constructed a core database of the Zuidwending cavern field and assigned the stratigraphic units and linked it to the list of available cores provided by TNO. Based on this, we pre-selected a significant part of cores to be inspected in further detail at the TNO core storage facility. At the core storage we examined more than 200 cores, roughly one-third of what is available, and selected 64 cores for 360° core scanning in at DMT in Essen. From earlier reports in this project, it is clear that the presence of megagrains and anhydrite fragments will have a major effect on the rheology of the rock salt at low differential stress and on the heterogeneity of permeation. After segmentation of the anhydrite and megagrains from the core scans and quantitative analyses we selected 30 cores for the slabbing. The slabs were photographed in transmitted and reflected light at high resolution, for identification of inclusions, grain size and deformation fabric, better than using the whole core, which has a damaged and smeared surface caused by drilling. Based on the slabs, we classified the core in three lithotypes, that together with the stratigraphic units provided guidance selecting the core pieces for the subsequent workpackages. We pre-selected 10 core pieces for permeation (ZW3.2), 15 for deformation (ZW2.2), and 4 for the Altaussee Mine (ZW2.3) experiments, respectively, together with a core piece selected for microstructural analyses (ZW1.2). In addition, the core slabs will also be investigated in greater detail in ZW1.2.

Overall, the core piece selection is a robust representation of the Zuidwending cavern field in terms of spatial distribution and stratigraphy for the limited amount of core pieces and available core material. The stratigraphic units form a good basis for defining the mechanical units for the geomechanical modelling, however we do note that not all of the significant mechanical units in the diapir have been accessed by coring.

[1] https://www.nlog.nl/nlog/requestData/nlogp/allBor/metaData.jsp?tableName=BorLocation&id=150300376

1 Introduction

The goal of this work package is the selection of 30 representative or typical core pieces for microscale analyses, integrated with deformation and permeation experiments. Many wells have been drilled in the Zuidwending cavern field between 1964 and 2018 (Table 1). Core material was available from 16 out of 24 wells at the TNO Central core sample storage, located at Zeist in the Netherlands. Originally about 1000 meters of core material were retrieved, based on the geological end of well reports and core images, however actually approximately 700 core boxes were present at the storage facility (List provided by TNO). This vast amount of material in combination with the relatively large number of wells required a more sophisticated selection procedure then compared to the Haaksbergen and Heiligerlee cavern fields. Hence, we aimed to first select at least 60 cores, approximately 10% of the available cores, for 360° image scanning as a basis of selecting the final 30 cores for the microstructural (ZW1.2) and experimental analyses (ZW2.1&2 and ZW3.1&2). Additionally, the final core selection was planned to be slabbed along the side of the core to generate sample twins for the microstructural analyses (slab) and experiments (remaining core). Overall, this novel procedure provides a larger and thus more representative amount of slab material. Besides, the core scans provide legacy image data that can be further investigated after the core material is consumed for the microstructural or experimental analyses. See Figure 1 and Figure 2 for an overview of the well location and a cross-sectional overview, respectively.

Table 1. Well list Zuidwending Cavern field. Core material was available from the underlined wells. Source: https://www.nlog.nl/datacenter/brh-overview

Start Date	Well-code	Well Target
25-10-1964	ZWD-KNZ-01	*Salt solution mining*
04-10-1967	ZWD-KNZ-02	*Salt solution mining*
09-11-1967	ZWD-KNZ-03	*Salt solution mining*
02-07-1968	ZWD-KNZ-05	*Salt solution mining*
29-07-1968	ZWD-KNZ-04	*Salt solution mining*
20-01-1969	ZWD-KNZ-06	*Salt solution mining*
15-02-1969	ZWD-KNZ-07	*Salt solution mining*
26-05-1988	<u>ZWD-KNZ-08</u>	*Salt solution mining*
20-10-1988	<u>ZWD-KNZ-09</u>	*Salt solution mining*
10-02-2007	<u>ZWD-A4A</u>	*Gas storage*
14-02-2007	<u>ZWD-A2A</u>	*Gas storage*
20-04-2007	<u>ZWD-A4B</u>	*Gas storage*
29-04-2007	<u>ZWD-A2B</u>	*Gas storage*
09-06-2007	<u>ZWD-A3A</u>	*Gas storage*
05-08-2007	<u>ZWD-A3B</u>	*Gas storage*
16-09-2007	<u>ZWD-A6A</u>	*Gas storage*
09-11-2007	<u>ZWD-A6B</u>	*Gas storage*
09-07-2009	<u>ZWD-A7A</u>	*Gas storage*
06-09-2009	<u>ZWD-A7B</u>	*Gas storage*
28-10-2009	<u>ZWD-A1A</u>	*Gas storage*
03-01-2010	<u>ZWD-A5A</u>	*Gas storage*
24-02-2010	<u>ZWD-A5A-S1</u>	*Gas storage*
12-04-2010	<u>ZWD-A8A</u>	*Gas storage*
25-04-2018	ZWD-A1B	*Gas storage*

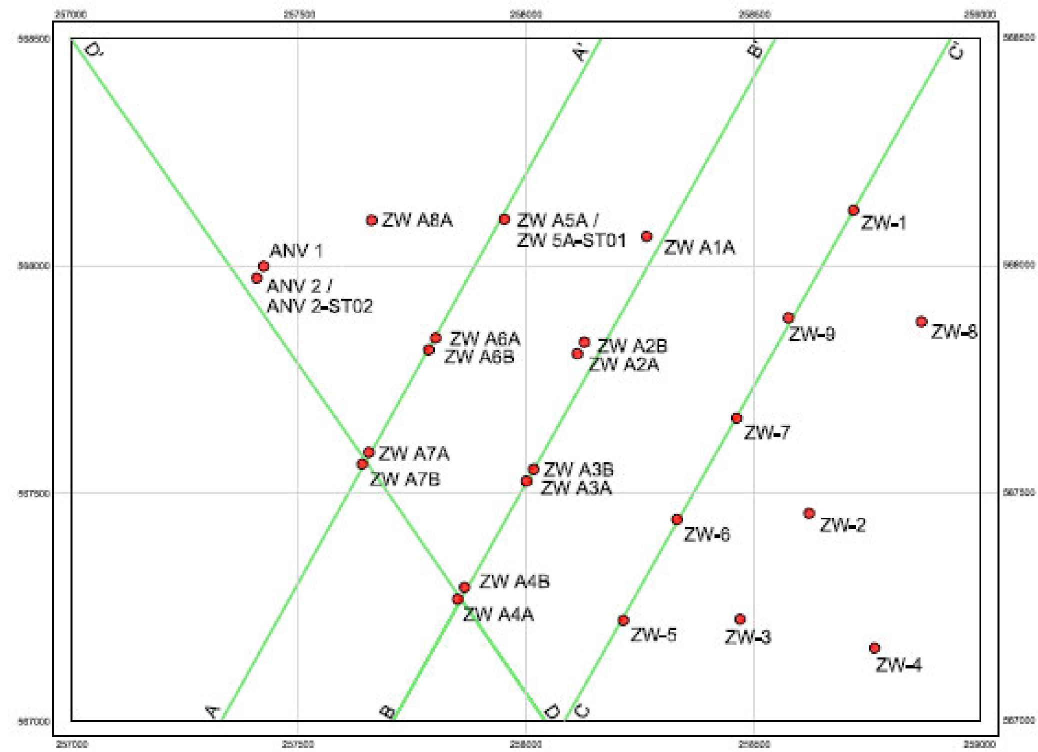

Figure 1. Overview of the well locations in the Zuidwending Cavern field, after Enclosure 4 in "Supplemental Report to the Digital Geological 3D Model of the North-Western Part of the Zuidwending Salt Dome" by DEEP.KBB (07a_report 3D Zuidwending.pdf).

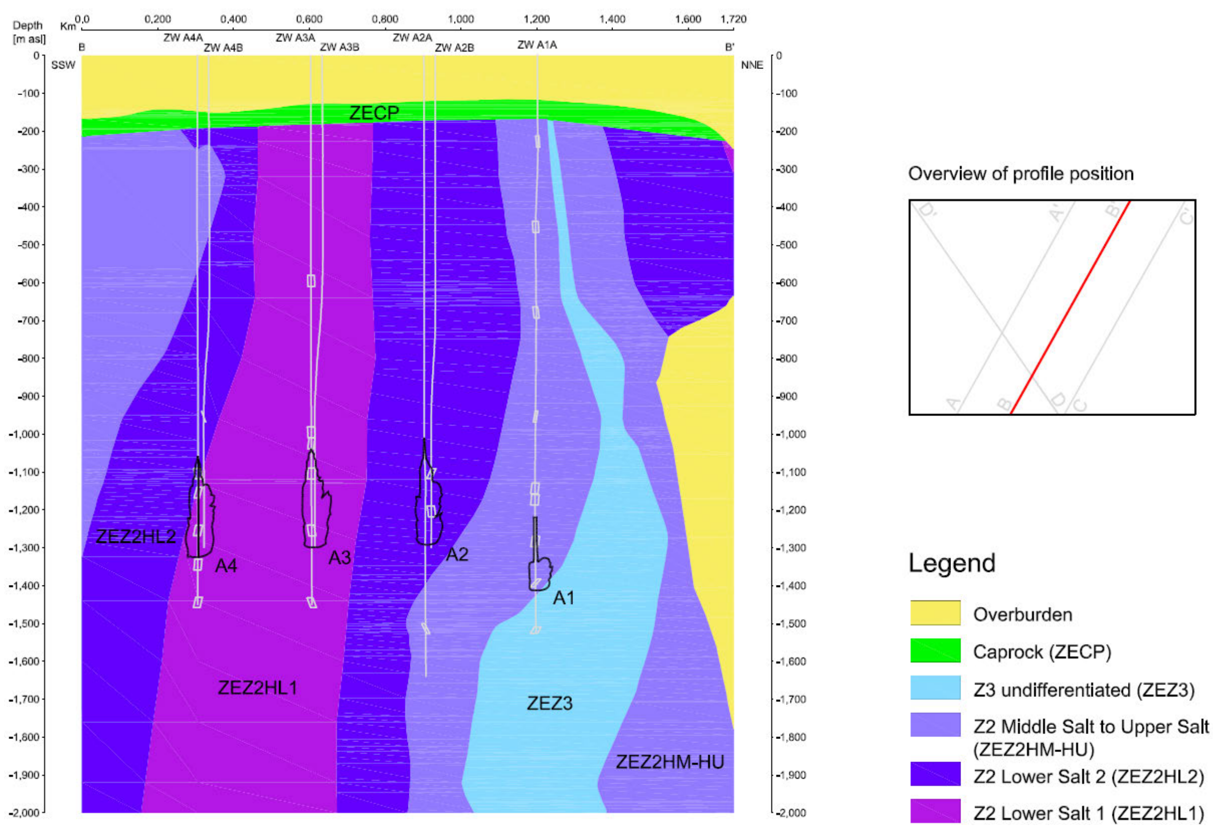

Figure 2. Cross-section B-B`after Enclosure 6 in "Supplemental Report to the Digital Geological 3D Model of the North-Western Part of the Zuidwending Salt Dome" by DEEP.KBB (07a_report 3D Zuidwending.pdf).

2 Methodology

2.1 Core pre-selection

At start of the project all available core images were documented and their properties were listed with as much detail as possible (e.g., core box depths, dip & azimuth, presence of anhydrite, degree of deformation, stratigraphic unit etc.). This database provided a first overview of the total material that was cored. Secondly, it potentially enables upscaling the current findings to the cores not investigated. After consultation with DEEP.KBB (07.02.2022) it was decided to pre-select the cores based on the stratigraphic units as described in "Supplemental Report to the Digital Geological 3D Model of the North-Western Part of the Zuidwending Salt Dome" by DEEP.KBB (07a_report 3D Zuidwending.pdf). Figure 3 and Figure 4 illustrate the depth distribution of the cores with respect to the different stratigraphic units in recent (after 2007) and older wells, respectively. However, as indicated in Table 1 not all cores from all wells were available in the core storage facility, moreover cores were taken for earlier or additional investigations by others (e.g., many cores from well ZWD-A5A and A8A were taken). Comparing our database with the list provided by TNO indicated about 600 meters of cores available at the storage facility (Table 2) which provided guidance at the storage facility as we aimed to select cores of each unit and each well.

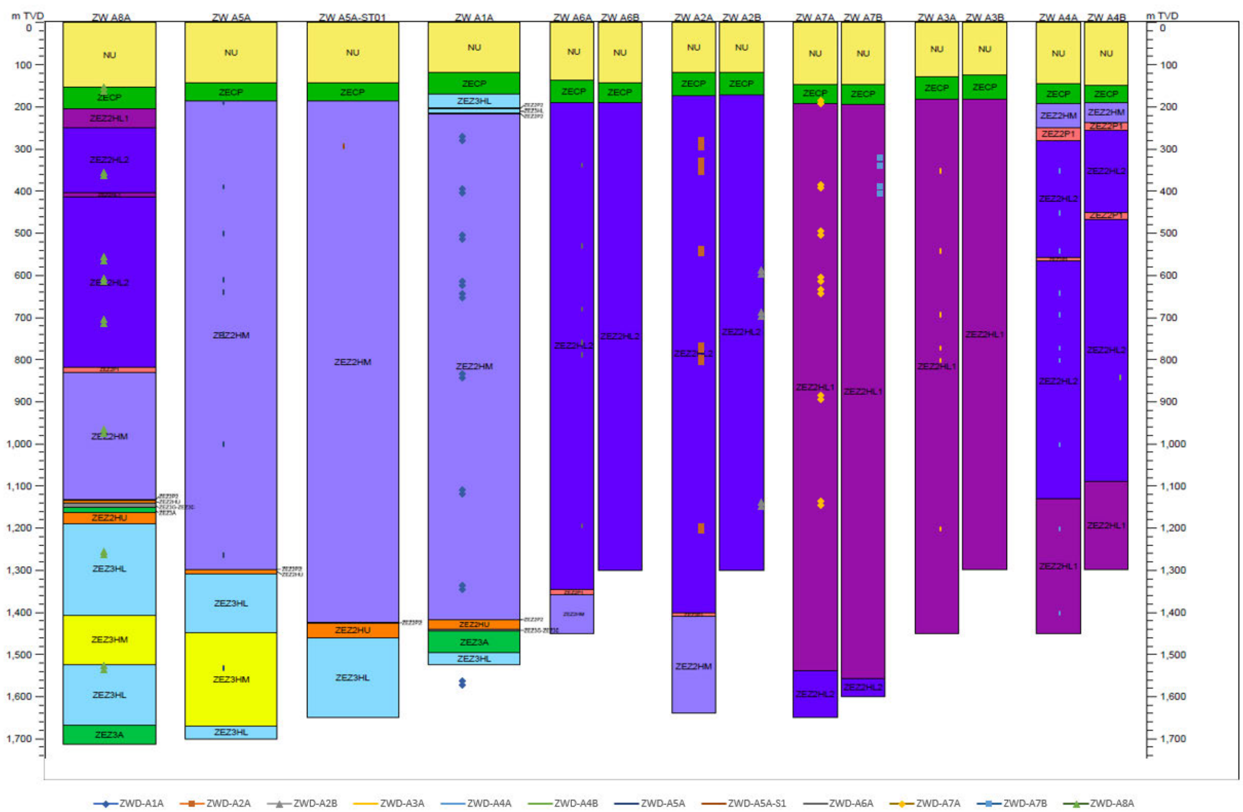

Figure 3. Stratigraphic columns and depth indication of the cores. Modified after Enclosure 1 in "Supplemental Report to the Digital Geological 3D Model of the North-Western Part of the Zuidwending Salt Dome" by DEEP.KBB (07a_report 3D Zuidwending.pdf).

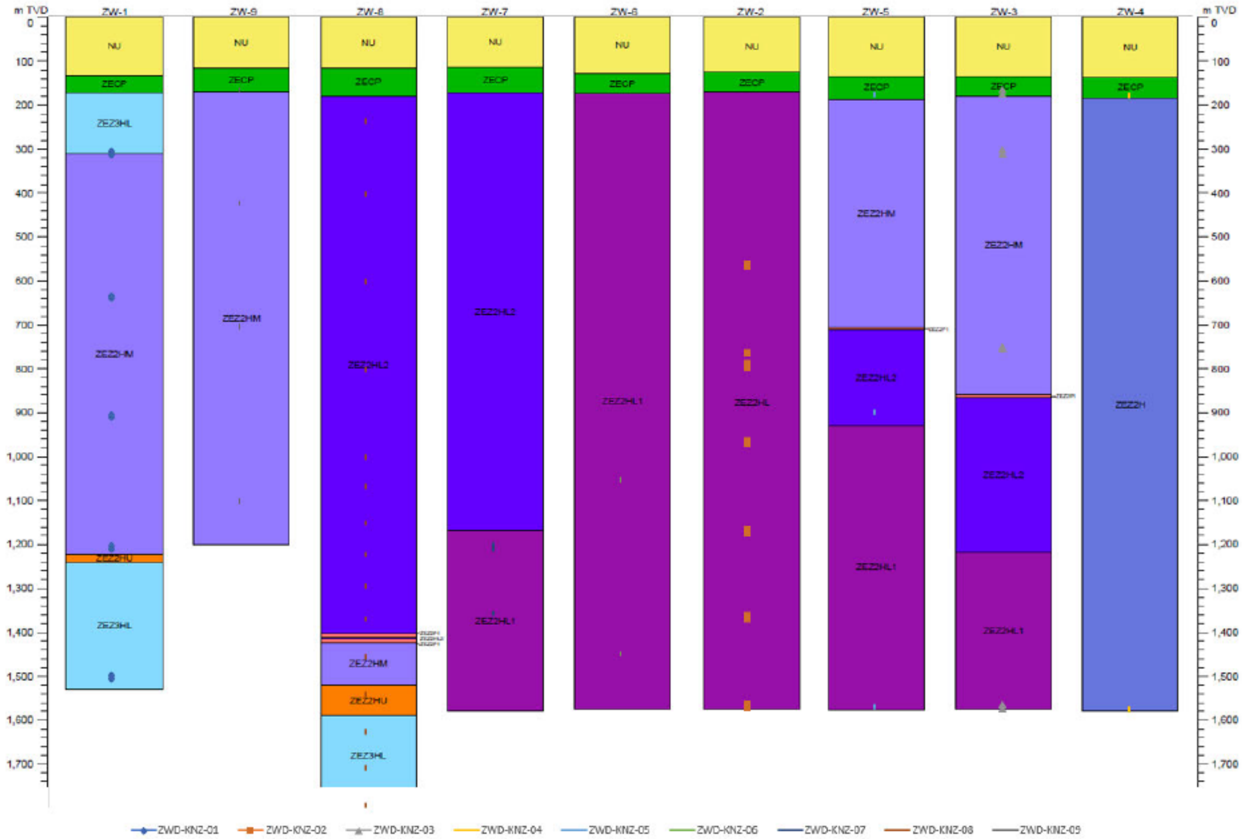

Figure 4. Stratigraphic columns and depth indication of the cores. Modified after Enclosure 2 in "Supplemental Report to the Digital Geological 3D Model of the North-Western Part of the Zuidwending Salt Dome" by DEEP.KBB (07a_report 3D Zuidwending.pdf).

Table 2. Indication of number of cores available at core storage facility of each unit and well (numbers are not exact as the provided list did not contain the exact depth ranges, complicating the comparison with our generated database).

	P0	ZEZ2HL1	ZEZ2HL2	ZEZ2HM	ZEZ3G/ZEZ3C	ZEZ3HL	ZEZ3HM	ZEZ3HU	Grand Total
ZWD-A1A				60		6			66
ZWD-A2A			25	38					63
ZWD-A2B			27						27
ZWD-A3A		37							37
ZWD-A4A		12	36						48
ZWD-A4B			7						7
ZWD-A5A				51					51
ZWD-A5A-S1						9			9
ZWD-A6A			35	9					44
ZWD-A7A		37	7						45
ZWD-A7B	12	16							28
ZWD-A8A			27	9	8				44
ZWD-KNZ-08			87			17	18	3	125
ZWD-KNZ-09				34					34
Grand Total	12	102	250	201	8	32	18	3	627

During the core storage facility visit (March 1 and 2, 2022) we examined and photographed about 1/3 of the available cores in various detail and the fraction of megagrains was estimated for a significant number of cores (n=145). Additionally, we pre-selected a sufficient number of cores that contained enough relatively fine-grained salt as required for the creep tests. Eventually we selected 64 cores in an iterative process the most suitable cores, meaning intact, not leached or fractured, and relatively clean. The selected cores were directly shipped by MaP for the core image scanning the subsequent days.

2.2 Core scanning

At DMT GmbH (Essen, GE) the cores were scanned with the CoreScan3 drill core scanner. It is equipped with a high-resolution Line Scan Camera (push broom) and scans the full drill core circumference (360°) with a pixel resolution of 100 µm (Figure 5). The acquired scan was imported in the DMT CoreBase logging software that manages (depth, and orientation if available) and enables visualization of the unrolled core or the reconstructed core in 3D and drawing bedding or fracture lineation's. The unrolled core images were further analysed in GIS to segment the megagrains and anhydrite. As the scans are actually cylindrical in shape, the amount of megagrains, anhydrite and matrix are corrected for the curvature by projecting the fractions of each line scan on a section perpendicular to the bedding. Based on these investigations and distribution of cores with respect to dept and stratigraphic unit the core selection was further down sampled from 64 to 30 cores. These cores were slabbed and the slabs and remaining cores will be used for the subsequent workpackages (ZW1.2, 2.1, 2.2, 2.3, 3.1 and 3.2).

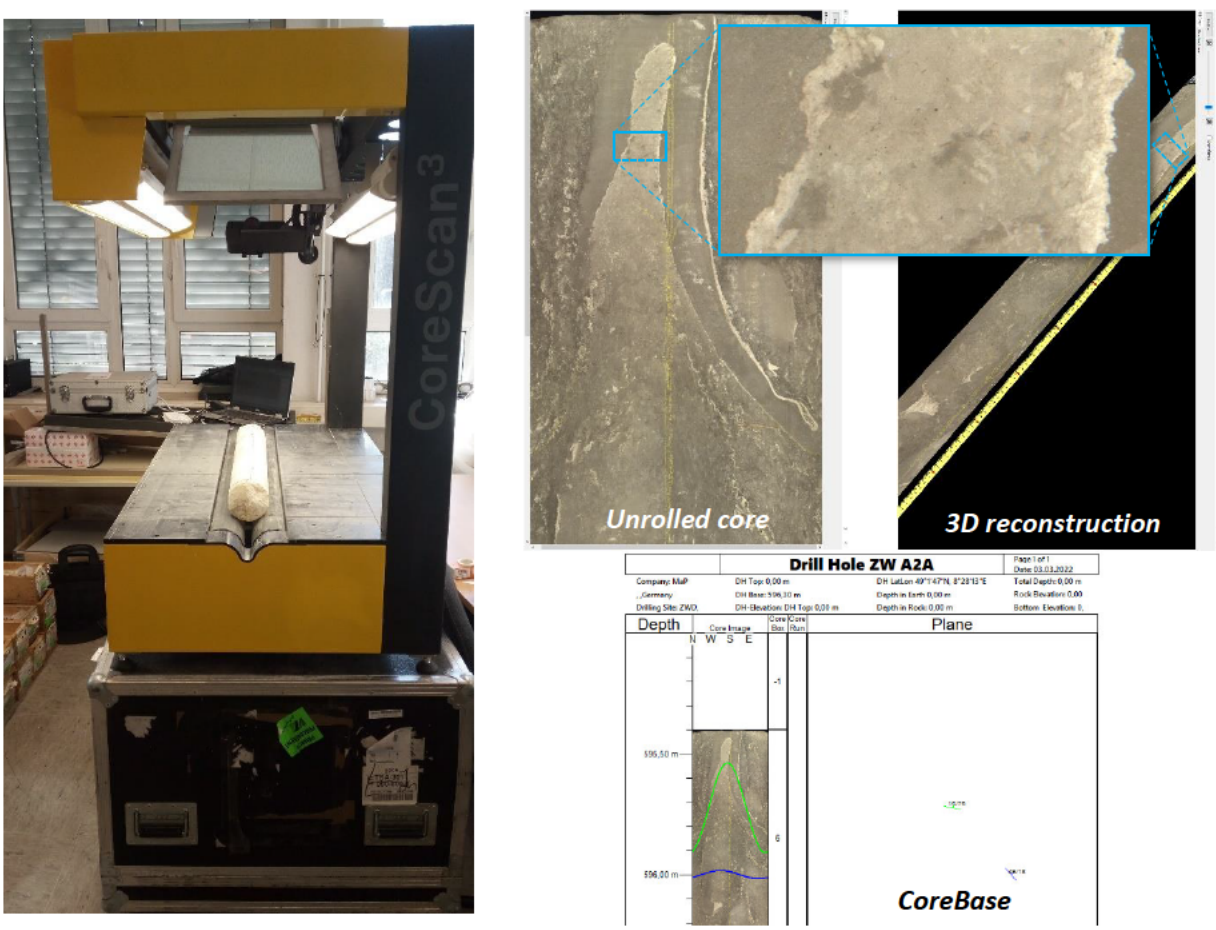

Figure 5. Picture of CoreScan3 drill core scanner with salt core (left) and screen shots of the unrolled core, 3D reconstruction and CoreBase logging software.

2.3 Core slabbing

The side perpendicular to the average orientation of the bedding was embedded in epoxy on a glass plate for each core (Figure 6) and cut the following day. Cores were cut with a rock saw equipped with a diamond saw blade (Ø 350mm, thickness 3mm) using saturated brine as a cooling agent. Directly after cutting the slab and remaining core were dried with tissues and hot air. In a next step the slabs and cores were photographed in transmitted and reflected light using Ipad Pro camera (pixelsize approximately 100µm). The mosaic images were stitched and imported into GIS for the segmentation of the megagrains and anhydrite.

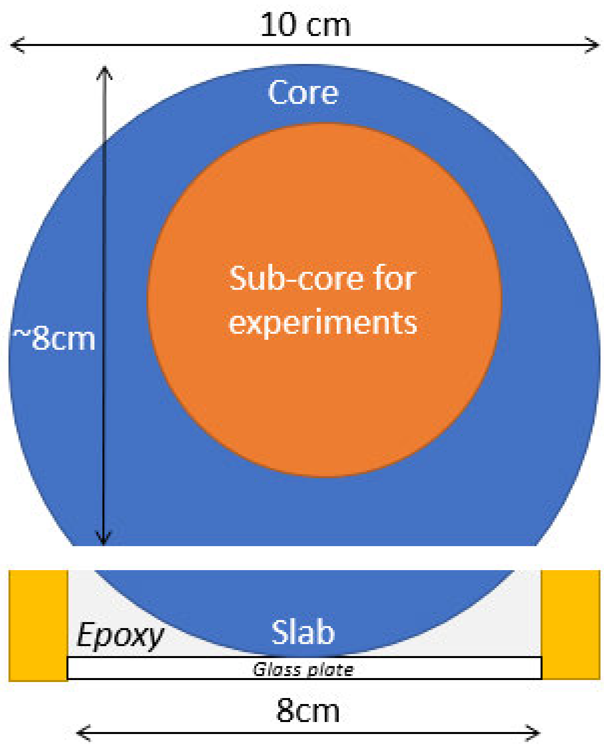

Figure 6. Sketch illustrating the slabbing with indication of the potential location of sub-core for subsequent experiments.

2.3.1 Nomenclature

For the qualitative and quantitative analyses core and slab description and analysis, we distinguished three different main phases in the salt slabs: anhydrite, polycrystalline halite, and extraordinarily large halite crystals or grains within the polycrystalline halite matrix. The latter is also known as the "Kristallbrocken" (e.g., Küster et al., 2010[2]), or halite mega-crystals (Report, Project KEM-17[3]). In the following we use the term megagrains to describe this feature, following the common definition of a "grain" in material science. The polycrystalline Halite can again be separated into fine- and coarse-grained lithologies, based on the observations of the salt slabs. The cores are named the following:

WellName_CoreNumber_CoreBox_TopCore(m).

[2] https://link.springer.com/article/10.1007/s00531-008-0399-8

[3] https://www.sodm.nl/binaries/staatstoezicht-op-de-mijnen/documenten/rapporten/2020/02/11/onderzoek-langetermijnrisicos-afsluiten-zotcavernes/KEM-17+Micro-scale.pdf

3 Qualitative description and quantitative analysis of core and slab composition and structures

3.1 General core description and core selection

Most of the salt cores contained megagrains mostly associated with thin anhydrite layers that are tilted, folded, off-set/juxtapose, bended or completely disrupted. The later ones can be considered as mylonitic fabric containing patches of boudins and micro folding that does not enable reconstruction of the initial sedimentary structure, often accompanied with a clear grainsize reduction and remnants of megagrains. In general, the megagrains can be very large, covering almost the whole core. In between the megagrains finer grained salt is present with various sizes. The estimated amount of megagrains is on average about 55%. Comparing the estimated fraction of megagrains with the qualitative estimate deduced from the core images of the geological end of well reports scales relatively well (Figure 7). This trend can be used for upscaling, after calibration with the actual fractions measured from the slab segmentations.

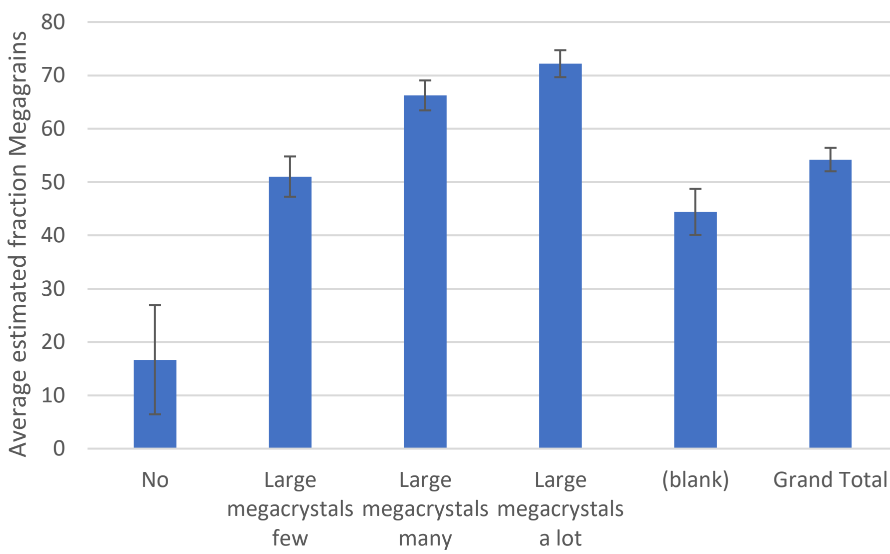

Figure 7. Average estimated fraction of megagrains versus the qualitative estimate deduced from the core images of the geological end of well reports. The core images labeled (blank) were of too low quality to interpret the amount of megagrains. The error bars are the standard errors.

Figure 8, Figure 9 Figure 10 show a random selection of images photographed at the storage facility at various scales illustrating the typical structures like folding with wave lengths varying from sub-centimetre to meter scale, often highlighted by a thin (few millimetres) anhydrite layer. Also, these thin layers are mostly accompanied by megagrains in case not completely deformed or recrystalized. The photographs also show that some of the cores are leached, broken-up or that core pieces are missing. Not shown on the images is that the core surface of many of the old cores (primarily from the ZWD-KNZ-08 and ZWD-KNZ-09 wells) were contaminated with dust. These observations also steered the selection as we preferentially selected intact, undamaged and clean cores for the microstructural analyses and deformation experiments. See the Appendix for more photos from the core storage facility visit.

ZWD_A2A_1_2_591.8

ZWD_A2B_1_7_655.1

ZWD_A4A_4_3_992.8

ZWD_A4A_5_10_1028

Figure 8. Photographs of salt cores inspected at the core storage facility.

ZWD_A6A_1_8_605

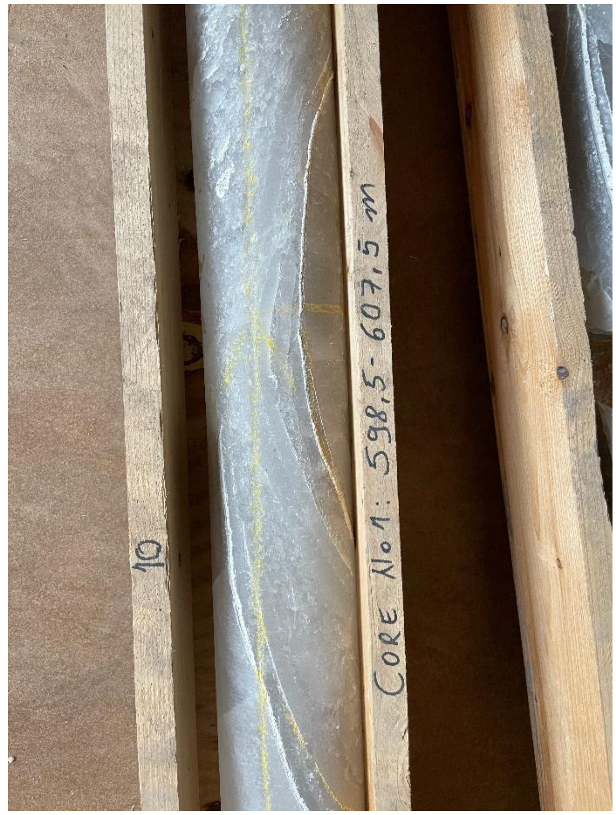

ZWD_A6A_1_10_606.8

ZWD_KNZ_9_2_7,6,9,11_425-430

ZWD_A8A_1,2_3,2,1_262,534-535.4

Figure 9. Photographs of salt cores inspected at the core storage facility.

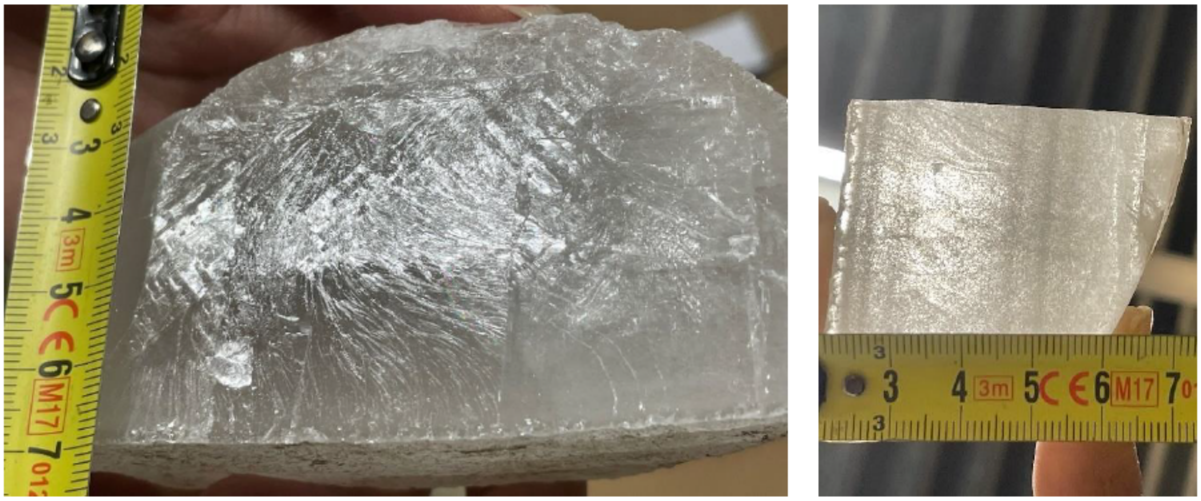

Figure 10. Detailed photographs of salt core pieces inspected at the core storage facility showing the thickness of megagrains. Left picture shows a cleavage crack surface in reflected light, showing small undulations representing subgrains. The right-side image shows the well-known layering inside the megagrains.

Table 3 shows the final core selection we selected for the core scanning. From each well, we selected core material and of about 10% of each stratigraphic unit was selected. The stratigraphic units of ZEZ3G/ZEZ3C and ZEZ3HU were not selected as they were very limited in number and not intact.

Table 3. Number of cores selected at core storage facility.

	P0	ZEZ2HL1	ZEZ2HL2	ZEZ2HM	ZEZ3HL	ZEZ3HM	Grand Total
ZWD-A1A				6	2		**8**
ZWD-A2A			2	3			**5**
ZWD-A2B			2				**2**
ZWD-A3A		5					**5**
ZWD-A4A		3	6				**9**
ZWD-A4B				4			**4**
ZWD-A5A					1		**1**
ZWD-A5A-S1			4	1			**5**
ZWD-A6A		1	1				**2**
ZWD-A7A	2	2					**4**
ZWD-A7B			2	1			**3**
ZWD-A8A			9		3	1	**12**
ZWD-KNZ-08				3			**4**
ZWD-KNZ-09				6	2		**8**
Grand Total	**2**	**11**	**26**	**18**	**6**	**1**	**64**
Fraction*	**14%**	**9%**	**9%**	**8%**	**16%**	**5%**	**9%**

**The fraction is an estimate as total number of each stratigraphic unit could not be determined exactly.*

3.2 Core scans, segmentation and slab selection

Figure 12 (next page) shows the unrolled scan of ZWD-KNZ-8 4_9_807 indicating the megagrains and anhydrite which were segmented in QGIS. The scans of all unrolled cores including the segmentations are presented in the Appendix and the fractions of anhydrite, megagrains and matrix are listed. Also, the mean bedding orientation (dip direction and dip, obtained from the DMT CoreBase software with respect to scan start) is given and used for correcting the segmented fraction for the curvature of the core. Below shows the variation in dip with depth of all scanned cores indicating that the main orientation of the layers is sub-vertical in the top and decreasing downwards, conform the main orientation of the stratigraphic units of the cavern field (Figure 11a). Plotting the fraction of megagrains with depth and stratigraphic unit does not show a clear trend (Figure 11b). The estimated content scales with the segmented amount of megagrains (Figure 11c). The overall average megagrain and anhydrite content from the core scans is 28% and 4%, respectively, with highest content of megagrains in the ZEZ2HL2 and ZEZ2HM stratigraphic units (Figure 11d). More specifically, the contents correspond to the descriptions of the units by DEEP.KBB.

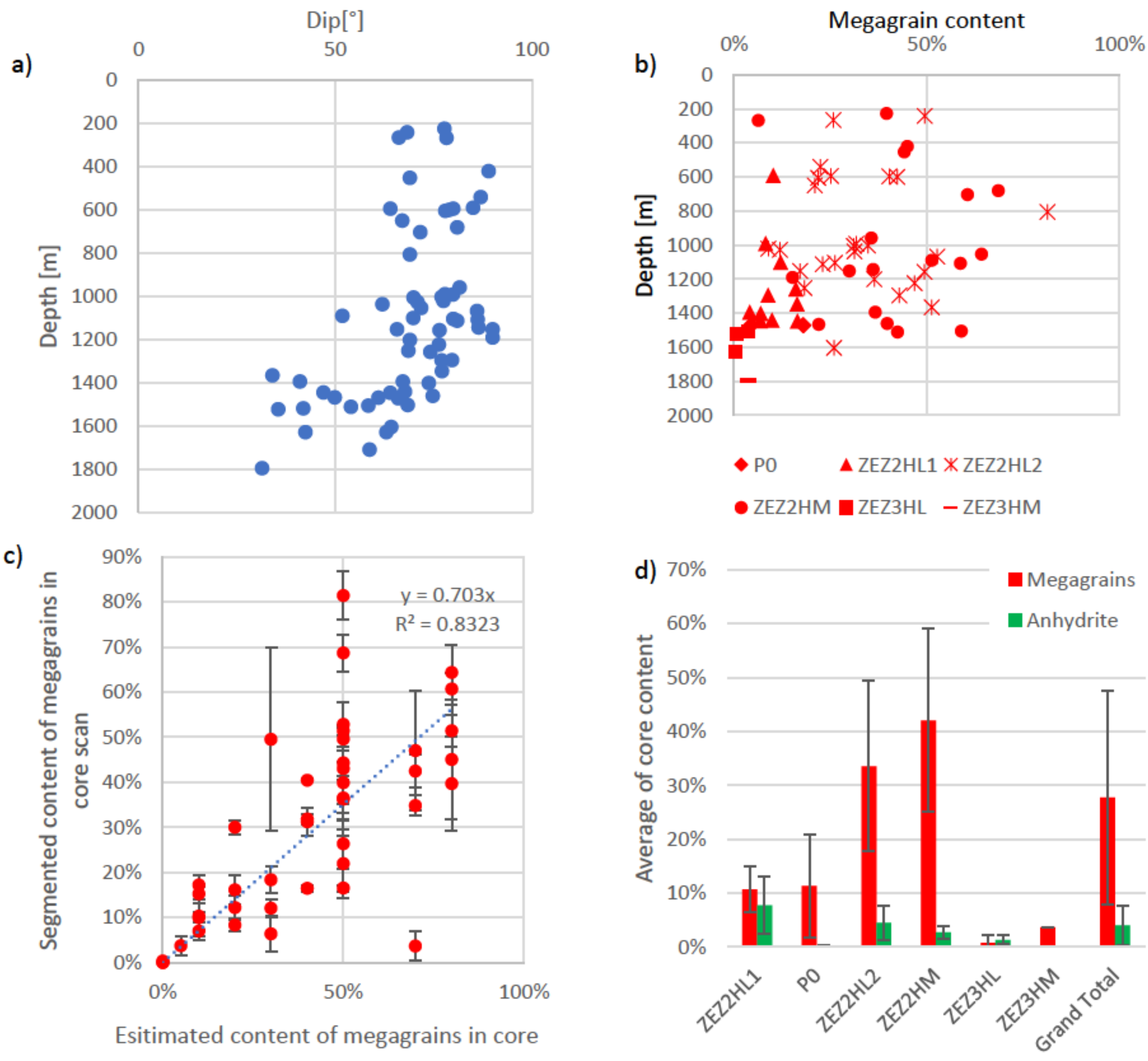

Figure 11. Quantitative core scan results. a) Dip versus depth b) Segmented megagrains versus depth for each stratigraphic unit. c) Segmented versus estimated megagrain content. D) Average content for each unit. The error bars are the standard deviations.

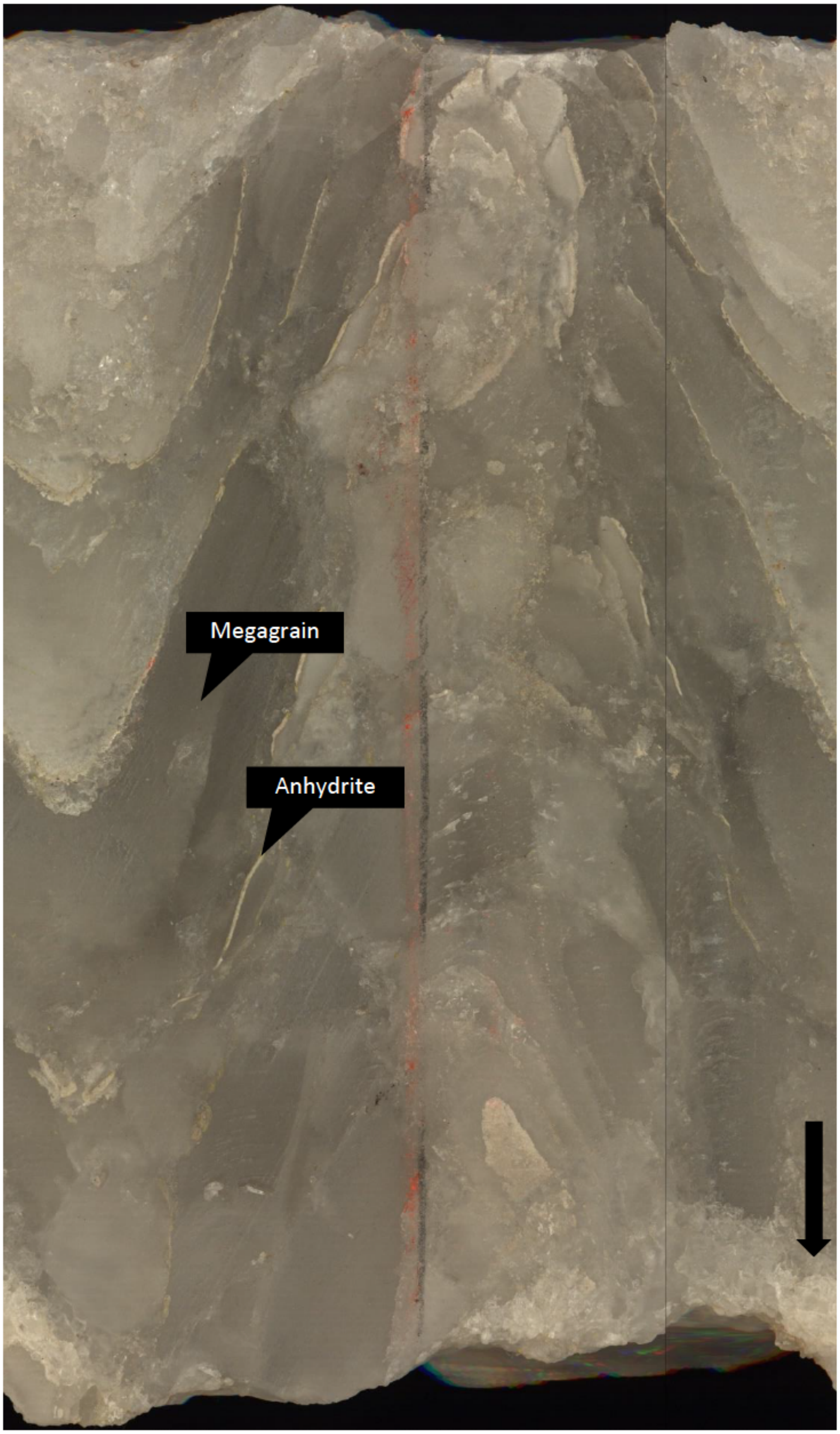

Figure 12. Unrolled core scan of ZWD-KNZ-8 4_9_807.16 indicating a megagrain and anhydrite.

Stratigraphic description (by DEEP.KBB[4]) of the main salt units:

- ZEZ2HL1: "The average anhydrite content is estimated with 5 to 8 % vol. The halite is mainly translucent, colorless to milky white, mainly medium to coarse grained and rarely occurs as large, platy monocrystals (up to 8 cm thick).
- ZEZ2HL2: "...characterized by rock salt of heterogranular texture with large, platy halite monocrystals floating in a medium to coarse grained matrix. The normally boudinaged monocrystals are up to 6 cm thick, typically bounded by thin anhydrite layers ... The overall anhydrite content of the ZEZ2HL2 is 4 to 7 % vol."
- ZEZ2HM: "as described for the upper part of the ZEZ2HL2... Throughout the unit, the abundance of large halite monocrystals increases while at the same time the anhydrite content decreases to amounts of between 5 and 2 % vol. near the top."

Eventually 30 cores were selected (Figure 13) from the 64 scanned cores for the subsequent slabbing according to the following selection criteria:

- 2 cores selected from comparable depth at start for the Mine experiments:
  - Including Megagrains → ZW A2A 8_7_1505.80 (ZEZ2HM)
  - Dominated in fine grained matrix → ZW A7B 1_13_1400.88 (ZEZ2HL1)
- 15 cores relatively low in megagrain content for the deformation and permeation experiments of each unit and depth range.
- Remaining 13 cores include core relatively rich in megagrains, and core from wells initially not selected to increase spatial distribution.
- The quality of the cores: ideally intact and long cores were selected and rather recent cores than old ones (e.g., ZW_A8A over ZWD-KNZ-8).

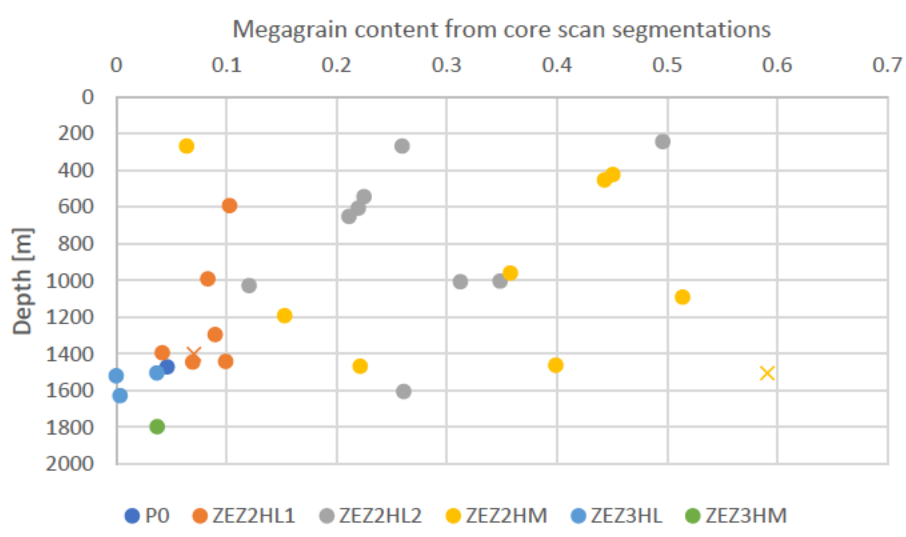

Figure 13. Overview of selected cores for the slabbing (and microstructural analyses and experiments in subsequent workpackages) with depth for each stratigraphic unit. The crosses are the cores selected and prepared for the Mine test.

[4] "Supplemental Report to the Digital Geological 3D Model of the North-Western Part of the Zuidwending Salt Dome" by DEEP.KBB (07a_report 3D Zuidwending.pdf).

3.3 Slab analyses and classification

The Appendix shows the segmentation and quantification of megagrain, anhydrite and halite matrix content of each slab in detail, as well as the slab type class.

The matrix consists of polycrystalline halite isometric in shape though elongated grains with weak preferred orientation are also present. The grainsizes ranges from few millimeters to few centimeters in size. The exact grainsizes will be determined in ZW1.2.

The halite megagrains are highly anisotropic up to 1 meter in length and few centimeters in thickness, mostly stacked, but are usually shorter because of the core orientation, boudinage and other deformation processes. The later results in megagrain remnants that are more isometric floating in the polycrystalline matrix.

The third phase, anhydrite, is the most distinct phase visible in the salt slabs due to its opaque character in transmitted light. The anhydrite occurred usually as thin layers (< 1cm) bordering the halite megagrains. Anhydrite is also visible as small anhydrite fragments or dust formed by small, fine-dispersed anhydrite grains or clusters of grains, but the thin layered anhydrite is dominant. The following sections describe the overall quantitative results and description of the core/slab type classifications.

3.3.1 Quantitative slab analyses

Figure 14a shows the average content of megagrain, anhydrite and halite matrix of each stratigraphic unit. Similar to the core scan segmentations, the stratigraphic units of ZEZ2HL2 and ZEZ2HM contain the highest content of megagrains. Generally, the slab megagrain content scales well with the megagrain fraction determined from the core scans (Figure 14b). The deviations are due to the fact that the slab section is at core side, while the average projected section from the core scan is through the middle of the core. Secondly, during segmentation occasionally smaller megagrains might be attributed to the matrix (coarse-grained) or visa-versa. Also, segmenting the megagrains from the reflected light core scans is not always straight forward, especially when they are not highlighted by anhydrite laminae or partly re-crystallized. Nevertheless, overall, the qualitative interpretation of megagrain content determined from the outside of the core images from the geological end of well reports is a relatively good proxy for a quantitative estimate of the megagrain content determined by the slabs (Figure 14c) which might be helpful for up-scaling scenarios in subsequent workpackages. The slab anhydrite content (Figure 14d) also follows the same trend as the core anhydrite content; however, the trend is not 1:1 and is attributed to over-segmentation of anhydrite from the core scans. Segmenting the anhydrite from the core scans is more difficult as only reflected light images are used, and core smearing is present on the core surface.

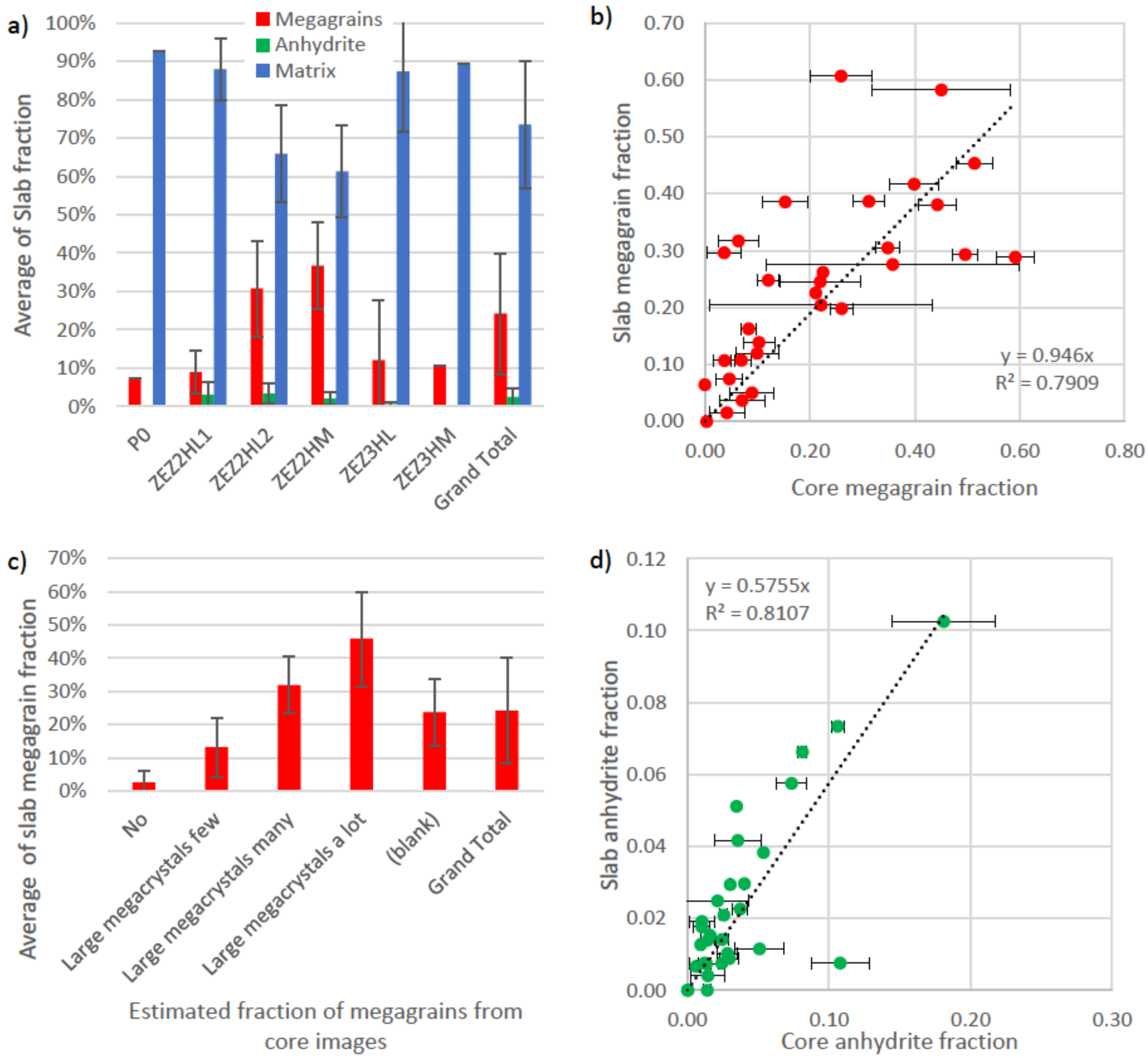

Figure 14. Quantitative results of the slab analyses. a) Average megagrain, anhydrite and halite matrix content of each stratigraphic unit. b) Comparison between megagrain content determined from the slab segmentation versus core scan segmentations. c) Comparison between anhydrite content determined from the slab segmentation versus estimated fraction of megagrains from core images. d) Average content of megagrains in the slabs versus the qualitative estimate deduced from the core images of the geological end of well reports. The error bars are the standard deviations.

3.3.2 Classification of the slabs (and cores)

The slabs can be classified based on the Heiligerlee lithotype classification (See HL1.1), though only partly. First of all, these slabs are about 4 times longer than the slabs prepared for the Heiligerlee cavern field and secondly much more core material was available of the Zuidwending cavern field compared to the Heiligerlee cavern field (only few tens of cores). As the slabs are so large, anhydrite layers are dominant over the anhydrite dust, hence lithotype class F was dominant over lithotype E and the later one was therefore not assigned. Due to the abundance of core material, cores relatively low in megagrain content were selected (preferred for the experiments) and therefore more lithotypes could be assigned, these are lithotypes G and H. Both are relatively low in megagrain content though the later one is dominated by mylonitic fabric. Figure 15a and b show the main quantitative characteristics of the different lithotype

classes in terms of megagrain and anhydrite content for each stratigraphic unit. The lithotypes are not restricted to a certain depth range (Figure 15c). The typical texture of each lithotypes is shown in Figure 16 in detail, the details of each slab can be found in the Appendix (slide 17-22). However, the overviews of the core and slabs in the Appendix show that a core or slab can actually be a mixture of two lithotypes. Here, only the most pronounced lithotype is presented or described which are further detailed in the next sub-sections. In the Appendix the secondary lithotype is written between parentheses. The cores which were not slabbed were also classified in retrospective.

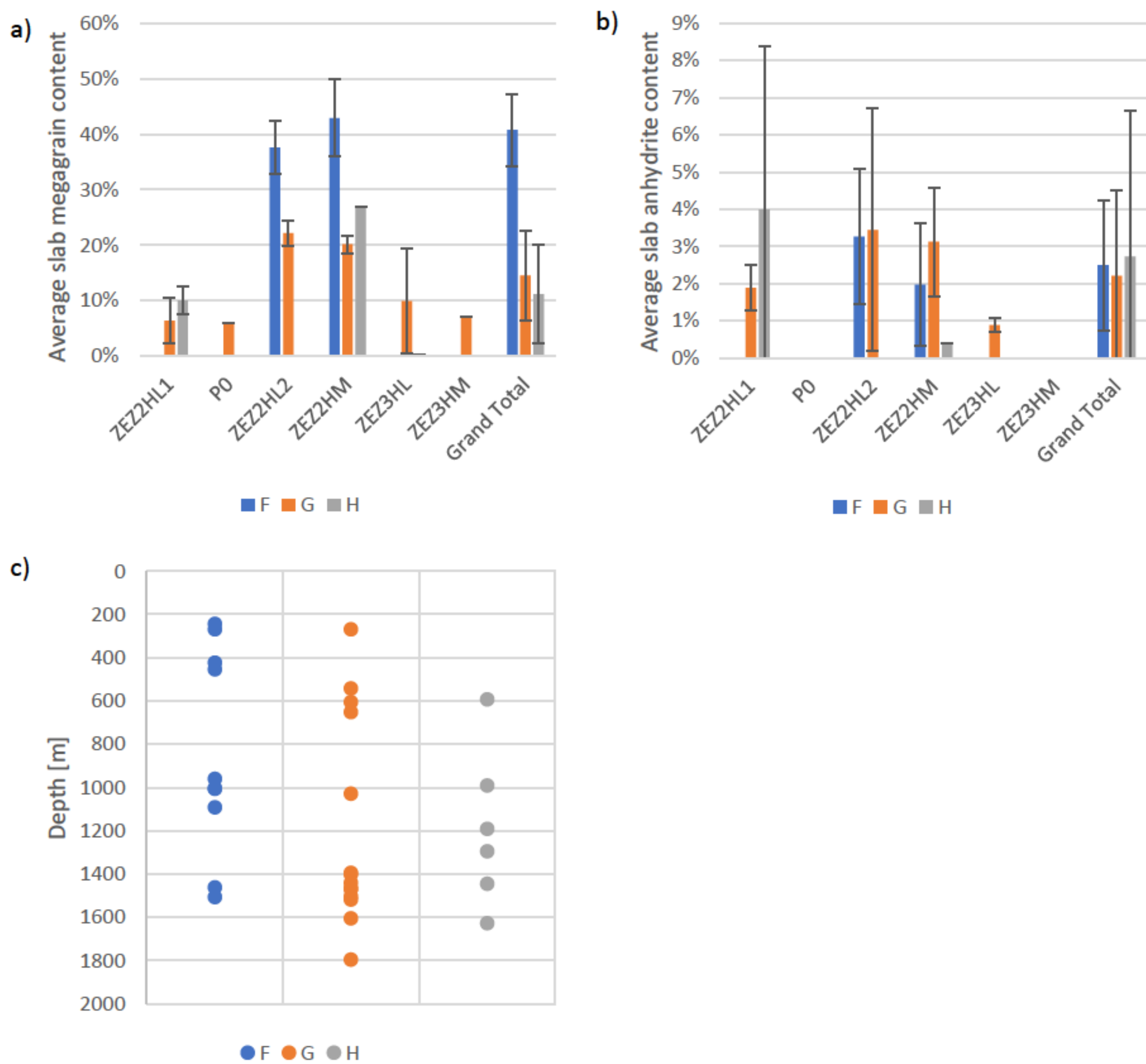

Figure 15. Average slab megagrain a) and anhydrite b) content of the different lithotypes for each stratigraphic unit and overall (Grand Total), error bars are the standard deviations. Depth distribution of the lithotype classes of all slabbed cores.

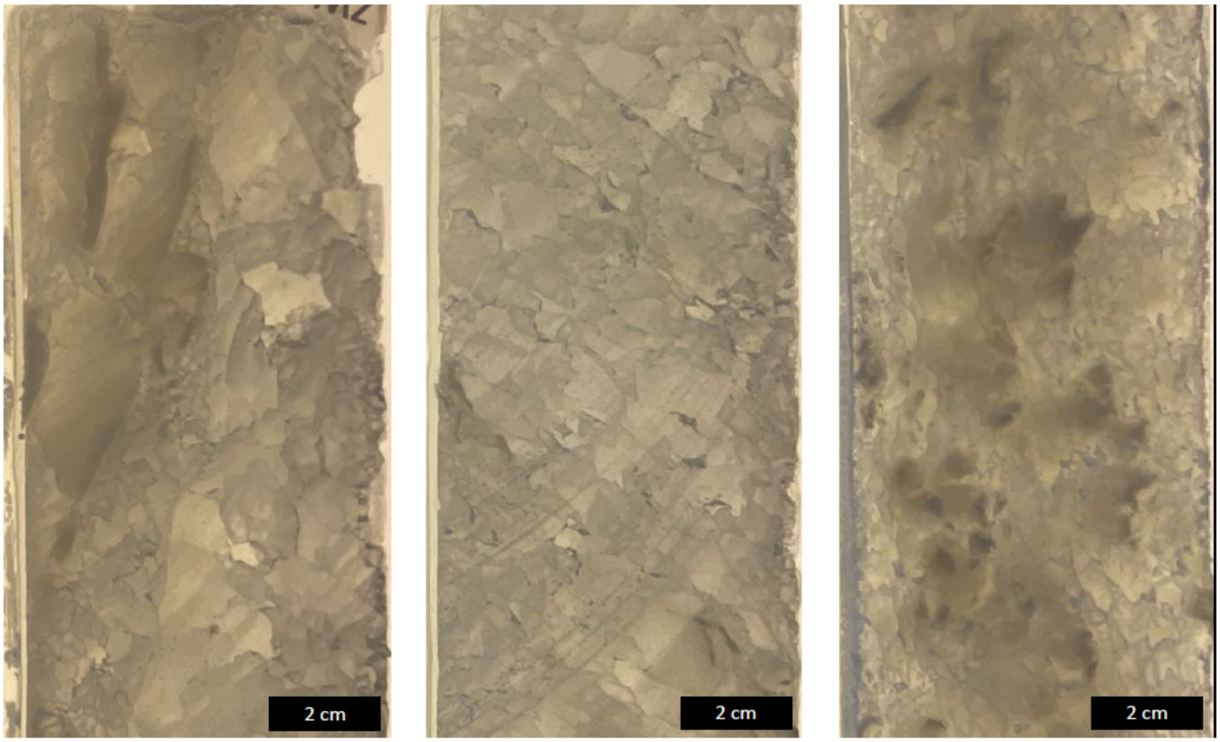

Class F: ZW A1A 4_7_0959.20_s (ZEZ2HM) H=17cm

Class G: ZW A1A 9_1_1518.00_s (ZEZ3HL) H=17cm

Class H ZW A3A 1_2_0591.90_s (ZEZ2HL1)

Figure 16. Typical texture of lithotype F, G and H.

3.3.2.1 Class F

Slabs classified with F (n=10) were in general very similar to the slabs classified for the Heiligerlee cavern field, especially the occurrence of thin anhydrite layers, often bordering the halite megagrains (Slide 17-18 Appendix). These anhydrite layers show small scale folding in some of the slabs (e.g., A28) and some of them were fractured and boudinaged (Slide 75 Appendix). The contact of the megagrains with the finer-grained halite matrix fraction was sometimes serrated, e.g., ZWD-KNZ-8 5_5_1003.13_s (Slide 117 Appendix), indicating recrystallization processes, this will be further discussed in ZW1.2. The megagrain and anhydrite content is on average 40.8% and 2.5%, respectively and this lithotype is dominant in the stratigraphic units of ZEZ2HL2 and ZES2HM (Figure 15). Cores with less than 25% of megagrains (average of core and slab megagrain content) were assigned to lithotype class G.

3.3.2.2 Class G

Slabs classified with G (n=14) consisted mainly of fine-coarse grained halite matrix with irregularly distributed anhydrite inclusions which appeared as isolated nodules or thin and shorth layers indicating the bedding orientation (Slide 20-21 Appendix). The common grain size of the equigranular, polycrystalline material was between 3 and 20mm. The grains are usually xenomorphic and isometric. Also, occasionally elongated grains with preferred orientation are present, indicating a foliation. Halite megagrain content is on average 14.5% and are mostly enclosed into the polycrystalline matrix. This lithotype class is present in all the stratigraphic units that was slabbed.

3.3.2.3 Class H

Class H contains the slabs with mylonitic fabric (n=6) containing on average the least amount of megagrains (11%) and a relatively highly variable halite matrix in terms of grain size and shape (Slide 22

Appendix). The core scan is also of help here as the bedding cannot be reconstructed, indicating intense deformation, also highlighted by the anhydrite patches. In the slabs the anhydrite is visible a dust or small nodules, especially in the ZEZ2HL1 stratigraphic unit, resulting in an average anhydrite content of 4.1%. An exception on these characteristics are the cores ZW A5A 6_9_1190.47_s (ZEZ2HM) and ZWD-KNZ-8 13_8_1627.58_s (ZEZ3HL) containing less anhydrite and rather a grain size reduction (Slide 78 and 124 Appendix).

3.3.2.4 Comparison to other cavern fields

The table below indicates the differences compared to the other cavern fields investigated in the HK1.1 and HL1.1. See the Supplement for a detailed description of the other core type classes. One has to consider that classification is not only scale depended but also orientation depended (core axis vs bedding orientation).

	Type	Short description	Difference compared to Zuidwending at slab scale
Haaksbergen	A	Almost pure salt core with Anhydrite dust and nodules	Class G contained on average hardly any anhydrite but more megagrains (<1% vs 2.5%, and 2% vs 14.5%, respectively).
Haaksbergen	B	Clear salt alternating with thick (> 5 cm) Anhydrite layers	Such thick and alternating anhydrite layers were not observed in Zuidwending.
Haaksbergen	C	Clear salt alternating with thin (< 5 cm) Anhydrite layers	Such alternating anhydrite layers were not observed in Zuidwending.
Haaksbergen	D	Dusty salt with a mylonitic fabric	Contained no megagrains, while in Zuidwending there is still about 11% of megagrains in class H
Haaksbergen	A & C	Almost pure salt core with Anhydrite dust and nodules and weak Anhydrite dust layering	-
Haaksbergen	B & D	Clear salt alternating with thick (> 5 cm) Anhydrite layers with deformed fabric	-
Heiligerle	E	Almost pure salt with Anhydrite dust and Halite mega-grains	Comparable to Class G Zuidwending, though average megagrain content significantly lower in Zuidwending (14.5% vs 24%).
Heiligerle / Zuidwending	F	Almost pure salt with thin Anhydrite layers at core scale and Halite mega-grains	Present in both Heiligerlee as Zuidwending. Also, anhydrite layers were dominant over dusty anhydrite and therefore Class E was not selected.
Zuidwending	G	Minor amount of megagrains (average of core and slab fraction <25%)	
Zuidwending	H	Mylonitic fabric	

4 Selection of sub-samples for microstructural analyses, deformation- and permeation experiments

4.1 Sub-sample selection for the Mine test

The core pieces for the mine test (Figure 17) were selected already at an early stage of the project (April 2022) and were selected based on the following criteria:

1. Experiment 1: one core piece rich in megagrains (plus one back-up sample)
2. Experiments 2-4: Three core pieces dominant in fine grained matrix (plus one back-up sample)
3. Core pieces from comparable depth to enable comparison

Core ZW A2A 8_7_1505.80 (ZEZ2HM) was selected for the megagrain creep test (experiment 1) as it is rich in megagrains (Slide 44 and 45 Appendix). Core ZW A7B 1_13_1400.88 (ZEZ2HL1) was selected for the mine creep tests on fine-grained halite as this one is relatively fine-grained and homogeneous (Slide 99 and 100 Appendix).

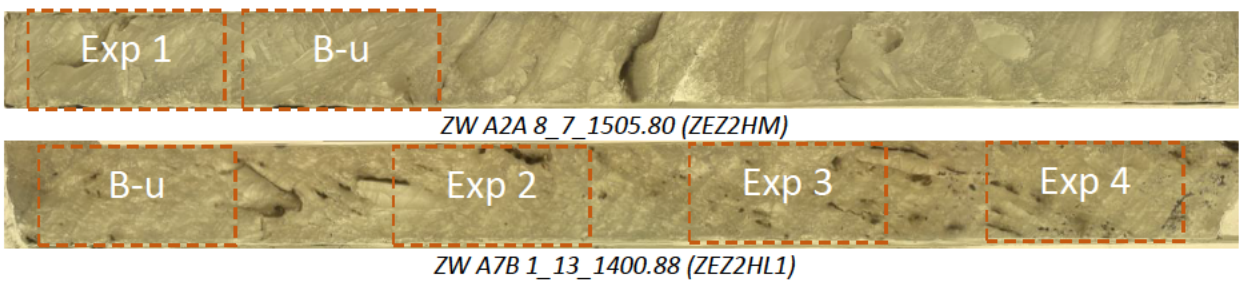

Figure 17. Slab photographs in transmitted light of the corresponding cores selected for the Mine tests with indication of the adjacent core piece selected for the 4 experiments (B-u = back-up sample).

4.2 Sub-sample selection for IFG

The core pieces for the deformation and permeation experiments were selected based on the slab composition and textures following these criteria:

1. Aim to sample at least each unit at various depths. Sampling each well is less important
2. Select ~5 coarse-grained and ~5 fine-grained, and ~5 core pieces with few mega grains for the deformation experiments
3. Select 10 core pieces relatively poor in megagrains, ideally next to a core piece selected for the deformation experiments.
4. One set of back-up core pieces

At first, core pieces of the stratigraphic units P0 and ZEZ3HM (2) were selected. Subsequently, core pieces dominant in coarse-grained matrix were selected (4, see slide 17-22 in Appendix with indication of coarse-grained halite fabric). In the next step the remaining 9 fine-grained samples, with half of them containing few megagrains, were selected in an iterative process making sure that all stratigraphic units were sampled covering all depth ranges avoiding high megagrain contents. Figure 18 shows the depth distribution of the selected core pieces for each stratigraphic unit. Table 4 also indicates the lithotype, experiment type and short core piece description. See the photograph of the cores in the Appendix for the exact location of the various core pieces indicated by purple and yellow polygons indicated in the Appendix for the permeation deformation experiments, respectively.

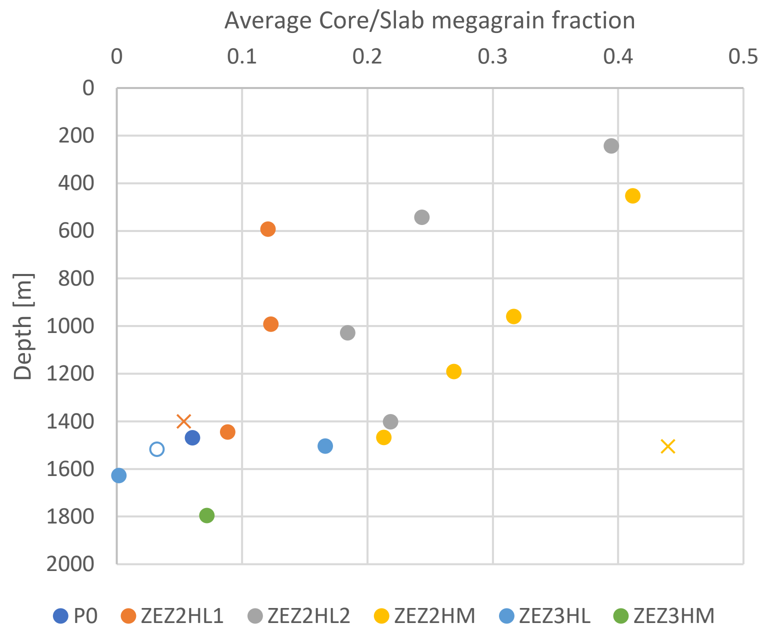

Figure 18. Overview of depths core pieces selected for the experiments. The crosses are the samples selected for the mine; the hollow marker is back-up material.

Table 4. Overview on selected core sample material for deformation (1 and 2) and permeation (2) experiments at IfG and the Altaussee Mine.

Well name	Core No.	Box slab No.	Top core box [m]	Strat. Unit	Lithotype	Exp.	Comment core sample
ZWD-KNZ-08	1	10	242.7	ZEZ2HL2	F	2	Fine (Megagrain remnants)
ZWD-A1A	2	2	452.62	ZEZ2HM	F	2	Fine
ZWD-A8A	2	9	542.23	ZEZ2HL2	G	1	Fine (Megagrain remnants)
ZWD-A3A	1	2	591.88	ZEZ2HL1	H	2	Fine (Mylonitic)
ZWD-A1A	4	7	959.2	ZEZ2HM	F	2	Coarse
ZWD-A3A	2	1	991.00	ZEZ2HL1	H	2	Fine (Mylonitic)
ZWD-A4A	5	10	1,028.00	ZEZ2HL2	G	2	Fine
ZWD-A5A	6	9	1,190.47	ZEZ2HM	H	1	Coarse (Megagrain remnants)
ZWD-A7B	1	13	1400.88	ZEZ2HL1	G	Mine	Fine
ZWD-A3A	6	5	1,444.51	ZEZ2HL1	H	2	Fine (Mylonitic)
ZWD-A2B	1	2	1400.88	ZEZ2HL2	G	1	Fine
ZWD-A2A	7	9	1467	ZEZ2HM	G	1	Coarse
ZWD-A7B	2	15	1469.27	P0	G	2	Fine
ZWD-A5A-S1	1	5	1503.26	ZEZ3HL	G	1	Coarse (Megagrain remnants)
ZWD-A2A	8	7	1505.8	ZEZ2HM	F	Mine	Megagrain
ZWD-A1A	9	1	1518	ZEZ3HL	G	2	Fine (Back-up)
ZWD-KNZ-08	13	8	1627.58	ZEZ3HL	H	2	Fine (Mylonitic)
ZWD-KNZ-08	15	6	1795.01	ZEZ3HM	G	2	Fine (Megagrain remnants)

4.3 Sub-sample selection for the microstructural analyses

A thin section from the slab of the mirroring part of each core that will be cut (Table 4) for the IfG deformation experiments will be prepared. On the contrary, a thin section will be prepared from the cores that are not selected for the IfG experiments. A selection of the slabs will be scanned at high resolution for further detailed analyses and comparison with the thin sections. Overall, each slabbed core will be investigated for microstructural analyses, see Figure 15c for their depths and lithotype classes. Approximately 5 core pieces selected for the thin-section analyses will be selected and prepared for the Gamma Irradiation experiments. These sub-samples still are under consideration but will at least include all lithotype classes and spread over the entire depth range.

5 Concluding remarks

This report describes the sampling procedure of 27 core pieces for analyses, experiments, and numerical models in the subsequent work packages, together with a qualitative description and quantitative analysis of core slab composition.

The core pre-selection was based on the core photographs in reflected and transmitted light available on the Nederlands Olie- en Gasportaal website and other provided material (Well report, the core photos and the core description) as well as on the discussion with DEEP.KBB to focus on the stratigraphic units as described in "Supplemental Report to the Digital Geological 3D Model of the North-Western Part of the Zuidwending Salt Dome" by DEEP.KBB (07a_report 3D Zuidwending.pdf). Based on this information 64 cores were selected, approximately 10% of what was available, covering the main stratigraphic units and cored wells that were present, forming a robust representation in terms of spatial distribution and structure of the Zuidwending cavern field. This core collection was scanned 360°, investigated and interpreted upon 30 cores were selected for the slabbing and subsequent core piece selection for the other workpackages.

Slab-scale analyses allowed distinguishing three dominant phases quantitatively: anhydrite, fine to coarse-grained polycrystalline halite, and halite megagrains (`*Kristallbrocken*`). Based on the slabs, we classified the core in three lithotypes, which provided guidance for selecting the core pieces for the microstructural analyses and experiments. Class F is rich in halite megagrains and often bounded by thin anhydrite layers. This lithotype was earlier described for the Heiligerlee cavern field (Heiligerlee Report WP1.1 210902). Class G is lower in halite megagrains content, a boundary was set at 25%, consisting mainly of fine to coarse-grained halite matrix with irregularly distributed anhydrite inclusions. Cores of class H dominate in mylonitic fabric. Based on the abundance of these lithotypes, it cannot be excluded that these are also present at Heiligerlee cavern field. However, the mechanical units for the geomechanical modelling rather sticks to the stratigraphic units indicated by DEEP.KBB.

We selected in total 15 (plus 1 spare) core sections for deformation experiments and 10 (plus 1 spare) core sections for permeation experiments at IfG (WPs 2.2 and 3.2). These core pieces cover all stratigraphic units that were available and spanning over a large depth range. Additionally, 4 (plus 2 spare) core sections were selected for deformation experiments at the Altaussee Mine (WP2.3).

Finally, on the core slabs and slabbed cores we selected locations for thin sectioning, including 5 for Gamma-irradiation, for further analysis in WP1.2, and analysis of deformed and permeated samples (WP2.1 and WP3.1). Selected core pieces will be cut, photographed, documented, prepared for shipment to IfG summer 2022.

A complete overview of all selected cores, slabs, slab segmentations and selection of sub-samples for microscale analyses, deformation and permeation experiments is presented in Appendix A.

Appendix A

Appendix A provides additional details on the selection procedure and outcomes. It also contains the core scan and slab images, and their segmentations and results. This document is a separate file: ZW1.1 Report Appendix A_220824.pdf.

Appendix B

Appendix B lists all core box images that were collected (from *Geological end of well reports* provided by the Dutch NLOG website[5], or provided by Nobian) at the start of the project. This document is a separate file: ZW1.1 Report Appendix B_220824.pdf.

Appendix C

Appendix C displays all core images acquired during the core shed visit early March 2022. This document is a separate file: ZW1.1 Report Appendix C_220302.pdf.

[5] https://www.nlog.nl/kaart-boringen

Supplement

Haaksbergen core types (from HK1.1)

Class A

Cores classified with A consisted mainly (>99%) of pure Halite with irregularly distributed Anhydrite inclusions which appeared as isolated nodules or weak layers of horizontal to sub-horizontal orientation. These Anhydrite inclusions were rather composed of finely dispersed small Anhydrite grains than of bulk Anhydrite. The Halite was usually translucent, colorless and clear, as also described in the report by DEEP (01_110302 Encl 7 core description ISH-01rev00d). The common grain size of the equigranular, polycrystalline material was between 1 and 10mm. The grains were usually xenomorphic and isometric. In the finer-grained fraction, grains were occasionally elongated with preferred orientation, indicating a foliation. Rarely, extraordinarily large grains - here named Halite mega-grains - were enclosed into the polycrystalline matrix.

The ten different slabs assigned to class A consisted to 100 area% of Halite, from which 98area% was polycrystalline, with 59area% coarse-grained Halite and 39area% fine-grained Halite. Two area% percent of the slab were Halite mega-grains. Anhydrite was present in the slabs, however, in the form of very small, dispersed grains, which were below the resolution of the segmentation technique and will be further discussed in the next WP1.2. The fine- and the coarse-grained polycrystals only occurred in one of the slabs together. Cores in this class originated from depths of 708 to 713 m and of 795 to 846 m.

Class B

In Class B we grouped cores consisting mainly of Halite (97%) alternating with massive, >5 cm thick Anhydrite layers and alternating with Halite layers containing small, dispersed Anhydrite grains (a.k.a. dispersed Anhydrite dust, DEEP report, 01_110302 Encl 7 core description ISH-01rev00d), with horizontal to sub-horizontal layering at core scale as well as vertical layering caused by folding of the Anhydrite layers. At the slab scale, this class exhibited pronounced heterogeneity within the Halite and within the Anhydrite fractions. The polycrystalline Halite fraction was typically coarse-grained with overall equigranular, isometric grains. Halite mega-grains were present but were usually elongated and presumably partly affected by recrystallization processes (this will be further resolved in WP1.2). At the slab scale, the massive Anhydrite layers also had near vertically oriented branches. We observed Halite grains and layers that were enclosed into the Anhydrite, and also Halite filled veins with the Anhydrite layers. At the slab scale, it could be speculated that boudinage and mylonitic fabric were present, which will be further investigated in WP1.2.

The quantification of the segmented slab surfaces of the four slabs assigned to class B showed an average of 62area% of Halite and 38 area% of Anydrite. Halite with 52 area% coarse-grained polycrystalline Halite and 10area% Halite mega-grains. Only in one slab polycrystalline, both, fine- and coarse-grained Halite were present at the same time. In comparison to the other types, in these slabs, Anhydrite was abundant with 38area% on average. Besides the thick sub-horizontal layers some vertical layers were present. In addition, all four slabs showed a varying amount of Anhydrite fragments and dust. Three of the four slabs had Halite veins within the thick Anhydrite layers at a core depth of 661 and 678 m.

Class C

Cores and slabs classified with C were characterized by usually clear, translucent Halite layers of several tens of cm thickness alternating with thin (< 5cm) Anhydrite layers. Near the Anhydrite layers, the Halite was often dusty caused by small, dispersed Anhydrite particles. At the slab scale we identified both, fine- and coarse-grained polycrystalline areas, occasionally with weak elongated shape and preferred orientation of the grains within the fine-grained fraction. Remnants of mega-grains were rarely observed. Anhydrite layers identified at the slab scale were usually thinner than 1 cm, with horizontal to sub-horizontal bedding.

The quantitative analysis of the four different slabs assigned to class C showed an average of 98area% of Halite in total, with 96area% fine-grained polycrystalline Halite, 2area% coarse-grained polycrystalline Halite and 3area% of Halite mega-grains. The remaining 2area% were Anhydrite, which was present as thin sub-horizontal Anhydrite layers, layer fragments, and small, dispersed grains or clusters of grains. The depths of the related cores were at 678 to 717 m.

Class D

Cores classified with D consisted of pure Halite (99 %) including layers of Halite with small, dispersed Anhydrite grains or clusters, with horizontal to sub-horizontal bedding. The pure Halite layers were usually dusty. At the slab scale the Halite was fine-grained with grains of elongated shape and pronounced preferred orientation. Remnants of thin, fractured, sheared, and folded Anhydrite layers indicated a mylonitic fabric.

The quantitative analysis of the five different slabs assigned to type D showed an average of 97area% of fine-grained, polycrystalline Halite. The remaining 3area% were Anhydrite. The depths of the cores related to analyzed slabs were at 726 to 789 m and at 926 m.

Class A and C

Class C was characterized by the presence of thin Anhydrite layers alternating with the salt, clearly visible at the core scale and within the slabs. However, in some cases a weak Anhydrite layering was visible at the core scale but not clearly confirmed at the slab scale. Here, the alternating Anhydrite layers were rather made up of dispersed small Anhydrite grains within the Halite matrix, than of bulk Anhydrite (e.g., Fig. A185). Therefore, the respective slabs were sorted into the class A and C. All cores within this class were foliated, usually only visible in the fine-grained polycrystalline fraction, with elongated grains with preferred orientation. The orientation of the foliation was shallow dipping with respect to the long axis of the core.

With this regard, quantitative analysis of the six D slabs assigned to type A and C (Fig. 3) showed an average of 100area% of pure Halite, such as also observed in the slabs classified with A. The polycrystalline Halite fraction was 93area%, with 61area% fine-grained polycrystalline Halite and 32area% coarse-grained polycrystalline Halite. Halite mega-grains were present in two third of the slabs and covered on average 7area% of measured the slab surfaces. Small Anhydrite grains were present with sizes below the resolution of the segmenting method. This Anhydrite “dust” was present in four from six slabs. In this class A and C, four out of the six slabs showed the presence of both, fine- and coarse-grained polycrystalline Halite. Slabs represented in this class were from core depths of 877 to 919 m and only one slab originated from a core depth of 708 m.

Class B and D

Class B enclosed the cores that contained thick, massive (>5 cm), sub-horizontally but also vertically oriented Anhydrite layers. The vertical orientation of the Anhydrite resulted from larger scale folding of the formation. However, at the core- to slab scale these cores comprised also smaller scale folding of the

Anhydrite layers as well as mylonitic overprinting of the phases. Hence, the relevant slabs we additionally labeled with D, which is the class that comprises slabs with structures showing (at this scale) evident deformation features. At the phase boundaries of the Anhydrite. with the Halite, thin Anhydrite layers alternated with deformed Halite mega-grains and coarse- and fine-grained Halite polycrystals. In the case of the fine-grained Halite, a weak preferred shape and preferred orientation of the grains was visible. These thin Anhydrite layers were sometimes folded or boudinaged. The presence of large Anhydrite (several cm) fragments within the Halite matrix indicated fracturing and transport of fragments of the thicker (~5cm) Anhydrite layers. Still rather intact massive Anhydrite layers were crosscut by veins with Halite filling.

The quantitative analysis of the six different slabs assigned to class B and D showed an average of 58area% of Halite in total. With a share of 55area%the polycrystalline Halite made up the slim majority of the segmented slabs. From that, 46area% were polycrystalline, fine-grained Halite and 9 area% of coarse-grained Halite. Coarse-grained Halite was found only in one slab. In comparison, the remaining five slabs consisted of fine-grained Halite. The Halite mega-grains only comprised 3area% of the whole slabs, which is only represented by one slab. The remaining 42area% represent the average Anhydrite. The core depth of the slabs ranged from 936 to 965 m and one slab was at a core depth of 731 m.

Heiligerlee core types (from HL1.1)

Class E

Slabs of Class E were described as an almost pure salt core with Anhydrite dust and Halite mega-grains. The Halite had an overall bimodal grain size distribution, consisting of Halite mega-grains, unusually with a highly elongated shape with a thickness (shortest axis) of 3 cm and more, and a finer-grained polycrystalline fraction. Grain boundary structure of the polycrystals was ranging from nearly straight to interlobate. The contact or the mega-grains with the finer-grained Halite fraction was often serrated, indicating recrystallization processes. In some of the slabs, we observed Anhydrite fragments along the grain boundaries or small dispersed Anhydrite grains distributed within the polycrystalline matrix.

The quantitative analysis of the eight different slabs assigned to Class E showed about 98 % of Halite, 65 % coarse-grained Halite and 9 % fine-grained Halite. The Halite mega-grains made up about 24 % of the total slab surface. Anhydrite was about 2 % in this class. Three out of eight slabs showed weak to no Anhydrite dust, whereas the remaining slabs showed this feature more clearly at macroscopic scale. Weak preferred shape of the polycrystalline halite was noted in a fifth of the slabs, with varying intensity. In addition, the coarse-grained Halite was visible in all eight slabs, whereas the polycrystalline fine-grained Halite was weakly represented in four slabs. Furthermore, two of the eight slabs only showed a very small amount of the Halite mega-grains.

Class F

Slabs classified with F were in general very similar to the slabs classified with E, especially regarding the size and morphology of the finer-grained Halite fraction. The main difference was the occurrence of thin Anhydrite layers, often bordering the Halite mega-grains. These Anhydrite layers recorded small scale folding in some of the slabs and some of them were fractured and boudinaged. The contact of the mega-grains with the finer-grained Halite fraction was sometimes serrated, as also observed in class E, indicating recrystallization processes, however, only in cases with minor Anhydrite or in the vicinity of small-scale Anhydrite folds.

The quantitative analysis of the ten slabs assigned to class F showed about 94 % of Halite. With 56 % the polycrystalline Halite made up the major proportion of the segmented slab surfaces. From that, 32 % were coarse-grained Halite and 24 % fine-grained Halite. The Halite mega-grains made up 38 % of the slabs. The remaining 6 % consisted of Anhydrite, which was present as thin sub-horizontal Anhydrite layers, dust and small fragments. Five of the slabs showed vertical layers or folds of Anhydrite, while, in three, Anhydrite fragments were present. In comparison, Anhydrite dust in form of small, dispersed Anhydrite grains was abundant in nine slabs with varying intensity. We observed weak preferred shape and orientation of the Halite grains, also with varying intensity within the ten slabs. Only one of the slabs consisted only of polycrystalline coarse-grained Halite (next to the Halite mega-grains), whereas the remaining nine slabs showed both coarse- and fine-grained with varying proportions.

We note here that the differences between the two classes used here are to a large extent given by the similar sizes of the slabs and the Halite mega-grains, associated with fine Anhydrite layers surrounded by finer grained Halite. Based on the analyses so far, it is not clear if this classification will be also present at the larger scale.